# Schrödinger formulation of the nondipole light-matter interaction consistent with relativity

Morten Førre [1,*] and Sølve Selstø [2]

[1]*Department of Physics and Technology, University of Bergen, N-5020 Bergen, Norway*
[2]*Department of Computer Science, OsloMet – Oslo Metropolitan University, NO-0130 Oslo, Norway*

An alternative and powerful Schrödinger-like equation for describing beyond dipole laser-matter interactions and leading relativistic corrections is derived. It is shown that this particular formulation is numerically very efficient with respect to computational effort and convergence rate of the solutions. Furthermore, its nonrelativistic form turns out to be more compatible with relativity than what seems to be the case with the more common formulations of the nonrelativistic light-matter interaction. Moreover, the extension of this interaction form into the relativistic region preserves, to a large extent, the numerical efficiency. In this work, the formulation is applied to study beyond dipole corrections and relativistic corrections in multiphoton ionization of a hydrogen atom in the x-ray regime.

## I. INTRODUCTION

The question of how the magnetic component of some laser field actually alters the strong-field ionization of atoms and molecules is becoming increasingly important and goes hand in hand with the ongoing development of new extreme light sources. Recent experimental activity in the field has already provided valuable insight into this emerging area of research [1–9]. The theoretical modeling of the laser-matter interaction in the intense field regime is particularly challenging, primarily due to the fact that the celebrated dipole approximation is generally no longer applicable [10–16]. Furthermore, in the limit of very strong fields the validity of the usual nonrelativistic approximation ultimately breaks down and a relativistic treatment of the laser-matter interaction becomes necessary [17–33].

In the present work we outline a coherent and transparent theoretical model for handling beyond dipole (nondipole) and relativistic corrections effects on an equal footing. This derivation is based on the time-dependent Schrödinger equation and the energy-momentum relation. The resulting interaction Hamiltonian turns out to be very favorable, not only from a computational point of view, but also from the point of view of better understanding the transition between the relativistic and nonrelativistic regimes. The work can be summarized by the formulas (21) and (25) derived in Sec. II, for the nonrelativistic and relativistic interactions, respectively. The usefulness of these formulations is explicitly demonstrated by studying the ionization dynamics of atomic hydrogen by a short and intense x-ray laser pulse in a regime where the ordinary dipole approximation is inaccurate [34]. It is shown that the here proposed scheme completely outmatches the more standard formulations of the light-matter interaction when it comes to comparing the rate of convergence of the

calculations with respect to the number of angular momenta included in the calculations. Moreover, for ionization processes pertaining to the softly relativistic regime, the ability to replace fully relativistic equations, i.e., the Dirac equation and the Klein-Gordon equation, with a dynamical equation of Schrödinger form, is a very convenient one indeed from a computational point of view. This is due to the fact that the numerical solution of the fully relativistic equations is complicated by numerical challenges such as severe stiffness and spurious states, from which the Schrödinger equation does not suffer.

Atomic units (a.u.) are used where stated explicitly.

## II. THEORY

In the standard nonrelativistic approach, the wave function $\psi(\mathbf{r}, t)$ of a particle of mass $m$ and charge $q$, evolving in some laser field $\mathbf{A}$ and (Coulomb) potential $V$, is governed by the time-dependent Schrödinger equation (TDSE),

$$i\hbar \frac{\partial}{\partial t} \psi = H\psi, \qquad (1)$$

with the minimal coupling formulation of the light-matter interaction Hamiltonian,

$$H = \frac{p^2}{2m} + V - \frac{q}{m}\mathbf{A} \cdot \mathbf{p} + \frac{q^2}{2m}A^2. \qquad (2)$$

Here the Coulomb gauge restriction, $\nabla \cdot \mathbf{A} = 0$, has been imposed on the field. The vector potential $\mathbf{A}(\mathbf{r}, t)$ generally depends on both space and time coordinates and satisfies separately the wave equation. From a purely computational point of view, keeping the spatial dependence in the vector potential most often results in an intractable numerical problem. Therefore, and in order to simplify the calculations significantly, the so-called dipole approximation is most often imposed. In this approximation the spatial dependence of the field is not considered, the magnetic field component is

_____
*morten.forre@uib.no

neglected, and the vector potential $\boldsymbol{A}$ is assumed to depend on time only. One consequence of the approximation is that the last (diamagnetic) term in the Hamiltonian (2) becomes an unimportant time-dependent factor that can be left out. The dipole approximation is usually valid in the limit where the extension of the quantum system in question is much smaller than the wavelength of the incoming light, provided that the laser intensity is not so high that the magnetic field component of the field must be included.

In an alternative and less known route, the system Hamiltonian can instead be written as [20,24,35,36]

$$H = \frac{p^2}{2m} + V - \frac{q}{m}\boldsymbol{A} \cdot \boldsymbol{p} + \frac{q^2}{4m^2c}\{A^2, \hat{\boldsymbol{k}} \cdot \boldsymbol{p}\}, \qquad (3)$$

where the unit vector $\hat{\boldsymbol{k}}$ indicates the laser propagation direction, $c$ is the speed of light, and curly brackets denote the anticommutator defined by $\{a, b\} = ab + ba$. The anticommutator originates from the fact that the two operators $A^2$ and $\hat{\boldsymbol{k}} \cdot \boldsymbol{p}$ do not generally commute. The interaction Hamiltonian (3) may also be obtained as the nonrelativistic limit of the Dirac equation—with the addition of the interaction between the particle's spin and the external magnetic field [37].

If we disregard terms beyond first order in $1/c$, the two formulations (2) and (3) are equivalent and can be used interchangeably, i.e., they would yield the same result in any exact treatment, provided the laser-matter interaction does not introduce relativistic effects. Nonetheless, the formulation (3), also called the *propagation gauge* formulation [35], has proven to be numerically advantageous in handling laser-matter interactions in the intense field limit where the dipole approximation breaks down [35,37]. The wave function $\psi'$ in the propagation gauge is related to the original wave function $\psi$ in Eq. (1) by the gauge transformation [35],

$$\psi' = e^{iX}\psi, \qquad (4)$$

with

$$X(\eta) = X(\omega t - \boldsymbol{k} \cdot \boldsymbol{r}) = \frac{q^2}{2m\hbar\omega} \int_{-\infty}^{\eta} A^2(\eta')d\eta', \qquad (5)$$

where $\omega$ is the central angular frequency of the laser field and $\boldsymbol{k} = \omega/c\,\hat{\boldsymbol{k}}$ is the wave vector.

In order to introduce the magnetic field in the standard formulation (2) of the light-matter interaction, it is common to write out the vector potential in terms of a Maclaurin series expansion, i.e., writing

$$\boldsymbol{A}(\boldsymbol{r}, t) = \boldsymbol{A}_0(t) + \frac{1}{c}\hat{\boldsymbol{k}} \cdot \boldsymbol{r}\boldsymbol{E}_0(t) + \dots, \qquad (6)$$

where $\boldsymbol{A}_0(t)$ now refers to the dipole field and $\boldsymbol{E}_0 = -\frac{\partial}{\partial t}\boldsymbol{A}_0$ represents the corresponding homogeneous electric field. In this approximation the magnetic field component is given by

$$\boldsymbol{B}(\boldsymbol{r}, t) = \nabla \times \boldsymbol{A} = \frac{1}{c}\hat{\boldsymbol{k}} \times \boldsymbol{E}_0 + \dots \qquad (7)$$

Applying the expanded potential (6), the minimal coupling Hamiltonian (2) is now cast into

$$H = \frac{p^2}{2m} + V - \frac{q}{m}\boldsymbol{A}_0 \cdot \boldsymbol{p} + \frac{q^2}{2m}A_0^2$$
$$- \frac{q}{mc}\boldsymbol{E}_0 \cdot (\boldsymbol{p} - q\boldsymbol{A}_0)\hat{\boldsymbol{k}} \cdot \boldsymbol{r} + \dots \qquad (8)$$

The performance of the Hamiltonian (8) in actual numerical calculations will be demonstrated later.

We will now go back and elaborate on the corresponding propagation gauge formulation (3). More specifically, we shall demonstrate that including spatial dependence in the $\boldsymbol{A} \cdot \boldsymbol{p}$ term in Eq. (2) or (3) may be problematic, both from a conceptual and a computational point of view.

For pedagogical reasons, we begin with showing how Eq. (3) can be derived. To this end, we take as starting point the relativistic minimal coupling Hamiltonian for a spinless particle of charge $q$ and mass $m$ confined in a (Coulomb) potential $q\varphi = V$ and interacting with some laser field $\boldsymbol{A}$,

$$H = \sqrt{m^2c^4 + (\boldsymbol{p} - q\boldsymbol{A})^2c^2} - mc^2 + V$$
$$= \frac{(\boldsymbol{p} - q\boldsymbol{A})^2}{2m} - \frac{(\boldsymbol{p} - q\boldsymbol{A})^4}{8m^3c^2} + \dots + V. \qquad (9)$$

Next, we impose the gauge transformation,

$$\boldsymbol{A} \rightarrow \boldsymbol{A}' = \boldsymbol{A} + \nabla\xi, \qquad (10)$$

$$\varphi \rightarrow \varphi' = \varphi - \partial_t\xi, \qquad (11)$$

on the potentials, with

$$\xi(\eta) = \xi(\omega t - \boldsymbol{k} \cdot \boldsymbol{r}) = \frac{q}{2m\omega} \int_{-\infty}^{\eta} A^2(\eta')d\eta'. \qquad (12)$$

Note at this point that this gauge transformation on the potentials is equivalent to the unitary transformation imposed on the system wave function in Eq. (4). The Hamiltonian (9) is then cast into its propagation gauge form,

$$H = \frac{\left(\boldsymbol{p} - q\boldsymbol{A} + \frac{q^2}{2mc}A^2\hat{\boldsymbol{k}}\right)^2}{2m} - \frac{\left(\boldsymbol{p} - q\boldsymbol{A} + \frac{q^2}{2mc}A^2\hat{\boldsymbol{k}}\right)^4}{8m^3c^2} + \dots$$
$$+ V - \frac{q^2}{2m}A^2$$
$$= \frac{p^2}{2m} + V - \frac{q}{m}\boldsymbol{A} \cdot \boldsymbol{p} + \frac{q^2}{4m^2c}\{A^2, \hat{\boldsymbol{k}} \cdot \boldsymbol{p}\}$$
$$- \frac{p^4}{8m^3c^2} + \frac{q}{4m^3c^2}\{\boldsymbol{A} \cdot \boldsymbol{p}, p^2\} - \frac{q^2}{8m^3c^2}\{A^2, p^2\}$$
$$+ \frac{q^3}{2m^3c^2}A^2\boldsymbol{A} \cdot \boldsymbol{p} - \frac{q^2}{2m^3c^2}(\boldsymbol{A} \cdot \boldsymbol{p})^2 + \dots, \qquad (13)$$

where in the last step only terms of order $(1/c)^2$ and lower have been written out explicitly. The Hamiltonian (13) in the present form also accounts for relativistic kinematic effects and was recently derived in [20,24]. Going to the nonrelativistic limit, i.e., omitting terms of order $(1/c)^2$ and higher, the nonrelativistic propagation gauge Hamiltonian (3) is finally retrieved.

Now, neglecting the spatial dependence of the vector potential, i.e., letting $\boldsymbol{A}(\boldsymbol{r}, t) \rightarrow \boldsymbol{A}_0(t)$ in Eq. (3), the Hamiltonian is converted into

$$H = \frac{p^2}{2m} + V - \frac{q}{m}\boldsymbol{A}_0(t) \cdot \boldsymbol{p} + \frac{q^2}{2m^2c}A_0^2(t)\hat{\boldsymbol{k}} \cdot \boldsymbol{p}, \qquad (14)$$

a form which is reminiscent of the interaction used in [38–41]. Already at this point one may notice one clear advantage of the propagation gauge formulation of the light-matter interaction in that the Hamiltonian (14) actually accounts for

magnetic field effects through the last term in the interaction [35], albeit no spatial dependence of the field has been retained. This stands in stark contrast to the standard minimal coupling formulation (2) for which the vector potential must be explicitly space dependent in order to account for the magnetic field; cf. Eqs. (6)–(8). The Hamiltonian (14) has yet another advantage in that in the limit of vanishing potential $V$, the momentum $\boldsymbol{p}$ becomes a constant of the motion, i.e., a conserved quantity. This is the main reason why the propagation gauge formulation in general tends to be more favorable from a purely numerical point of view, in particular in the limit of very strong perturbations.

As mentioned previously, including spatial dependence in the vector potential in the $\boldsymbol{A} \cdot \boldsymbol{p}$ operator term in the interaction Hamiltonian (2) or (3) may cause some trouble. Therefore, we are now about to introduce an additional unitary transformation to the light-matter formulation that will prove to be extremely useful in investigating intense field effects beyond the dipole approximation. To this end, we start out by writing out the Hamiltonian (3) on the following trivially extended form:

$$H = \frac{p^2}{2m} + V(\boldsymbol{r}) - \frac{q}{m}\boldsymbol{A}_0 \cdot \boldsymbol{p} - \frac{q}{m}(\boldsymbol{A} - \boldsymbol{A}_0) \cdot \boldsymbol{p}$$
$$+ \frac{q^2}{4m^2c}\{A^2, \hat{\boldsymbol{k}} \cdot \boldsymbol{p}\}, \tag{15}$$

where $\boldsymbol{A}_0 = \boldsymbol{A}_0(t)$ and $\boldsymbol{A} = \boldsymbol{A}(\boldsymbol{r}, t)$ as defined by Eq. (6). Next, the goal is to get rid of the $(\boldsymbol{A} - \boldsymbol{A}_0) \cdot \boldsymbol{p}$ term from the formulation. This may be achieved by introducing the unitary transformation,

$$\psi'' = U\psi', \tag{16}$$

to the propagation gauge wave function $\psi'$ in Eq. (4), with

$$U = \exp\left[\frac{i}{\hbar}\boldsymbol{\alpha}(\boldsymbol{r}, t) \cdot \boldsymbol{p}\right], \tag{17}$$

$$\boldsymbol{\alpha} = -\frac{q}{m}\int_{-\infty}^{t}(\boldsymbol{A} - \boldsymbol{A}_0)dt'. \tag{18}$$

The transformation will give rise to some new interaction terms which can be calculated using the Baker-Campbell-Hausdorff formula:

$$e^{ia}be^{-ia} = b + \frac{i}{1!}[a, b] + \frac{i^2}{2!}[a, [a, b]]$$
$$+ \frac{i^3}{3!}[a, [a, [a, b]]] + \dots. \tag{19}$$

The Hamiltonian from this new point of view becomes

$$H' = UHU^{\dagger} + i\hbar\dot{U}U^{\dagger}$$
$$= \frac{p^2}{2m} + V(\boldsymbol{r} + \boldsymbol{\alpha}) - \frac{q}{m}\boldsymbol{A}_0 \cdot \boldsymbol{p} + \frac{q^2}{4m^2c}\{A^2, \hat{\boldsymbol{k}} \cdot \boldsymbol{p}\}$$
$$- \frac{q}{2m^2c}\{\hat{\boldsymbol{k}} \cdot \boldsymbol{p}, \boldsymbol{A} \cdot \boldsymbol{p}\} - \frac{q^3}{2m^3c^2}A^2\boldsymbol{A} \cdot \boldsymbol{p}$$
$$+ \frac{q^2}{2m^3c^2}(\boldsymbol{A} \cdot \boldsymbol{p})^2. \tag{20}$$

The transformed Hamiltonian (20) contains in total three new terms that originate from the $(\boldsymbol{A} - \boldsymbol{A}_0) \cdot \boldsymbol{p}$ operator in Eq. (15).

In addition, the potential has been shifted, i.e., $V(\boldsymbol{r}) \rightarrow V(\boldsymbol{r} + \boldsymbol{\alpha})$.

At this point, the attentive reader may already have made the important observation that the last two terms in Eq. (20) are also present in the general relativistic Hamiltonian (13)—but with opposite signs. This means that when introducing the unitary transformation (16)–(18) to the relativistically extended formulation (13), all such terms happen to cancel exactly against each other, and therefore none of them should appear separately in any consistent model of the light-matter interaction, neither in the relativistic nor in the nonrelativistic limit. To this end, the formally correct (nonrelativistic) Hamiltonian takes the simpler form,

$$H = \frac{p^2}{2m} + V(\boldsymbol{r} + \boldsymbol{\alpha}) - \frac{q}{m}\boldsymbol{A}_0 \cdot \boldsymbol{p} + \frac{q^2}{4m^2c}\{A^2, \hat{\boldsymbol{k}} \cdot \boldsymbol{p}\}$$
$$- \frac{q}{2m^2c}\{\hat{\boldsymbol{k}} \cdot \boldsymbol{p}, \boldsymbol{A} \cdot \boldsymbol{p}\}. \tag{21}$$

We have here finally arrived at a relatively compact expression for the light-matter interaction. In this formulation the pure dipole interaction is represented by a separate term. In addition, the Hamiltonian contains three terms that are attributed to radiation of the electromagnetic field beyond the dipole approximation, i.e., the usual propagation gauge term proportional $A^2$, a new term proportional to $\boldsymbol{A}$ arising from the original $\boldsymbol{A} \cdot \boldsymbol{p}$ operator in Eq. (3), and finally, as a side effect of the transformation, the shifted potential $V(\boldsymbol{r} + \boldsymbol{\alpha})$. This modified potential may be expanded in ascending powers of $1/c$, i.e.,

$$V(\boldsymbol{r} + \boldsymbol{\alpha}) = V(\boldsymbol{r}) + \frac{q}{mc}\hat{\boldsymbol{k}} \cdot \boldsymbol{r} \, \nabla V(\boldsymbol{r}) \cdot \boldsymbol{A}_0 + \dots. \tag{22}$$

If we now settle for corrections of first order in $1/c$ to the light-matter interaction, we may keep only the leading order correction to the Coulomb potential as well as substitute $\boldsymbol{A}$ with $\boldsymbol{A}_0$ in the remaining two beyond dipole interaction terms. Then, the Hamiltonians (20) and (21) are cast into

$$H = \frac{p^2}{2m} + V - \frac{q}{m}\left[1 + \frac{\hat{\boldsymbol{k}} \cdot \boldsymbol{p}}{mc}\right]\boldsymbol{A}_0(t) \cdot \boldsymbol{p} + \frac{q^2}{2m^2c}A_0^2(t)\hat{\boldsymbol{k}} \cdot \boldsymbol{p}$$
$$+ \frac{q}{mc}\hat{\boldsymbol{k}} \cdot \boldsymbol{r} \, \nabla V \cdot \boldsymbol{A}_0(t) - \frac{q^3}{2m^3c^2}A_0^2\boldsymbol{A} \cdot \boldsymbol{p}$$
$$+ \frac{q^2}{2m^3c^2}(\boldsymbol{A}_0 \cdot \boldsymbol{p})^2, \tag{23}$$

and

$$H = \frac{p^2}{2m} + V - \frac{q}{m}\left[1 + \frac{\hat{\boldsymbol{k}} \cdot \boldsymbol{p}}{mc}\right]\boldsymbol{A}_0(t) \cdot \boldsymbol{p} + \frac{q^2}{2m^2c}A_0^2(t)\hat{\boldsymbol{k}} \cdot \boldsymbol{p}$$
$$+ \frac{q}{mc}\hat{\boldsymbol{k}} \cdot \boldsymbol{r} \, \nabla V \cdot \boldsymbol{A}_0(t), \tag{24}$$

respectively, and where $V = V(\boldsymbol{r})$ now refers to the unshifted potential. Note that the anticommutation rules in Eqs. (20) and (21) become unnecessary as $\boldsymbol{A} \rightarrow \boldsymbol{A}_0$ since the operators now commute, and they are therefore omitted in Eqs. (23) and (24).

The Hamiltonian (24), which contains all beyond dipole interaction terms up to and including order $1/c$ corrections, constitutes one of the main findings of the present work. The alternative formulation (23) is reminiscent of the light-matter

interaction derived recently by Brennecke and Lein [42], and which was used in explaining experimental data on magnetic field effects in the strong-field ionization of atoms [6]. In the nonrelativistic limit, and provided relativistic corrections of order $(1/c)^2$ and higher are unimportant to the dynamics, the two formulations (23) and (24) would yield similar but not identical results. Any discrepancy could then be attributed to the two extra terms appearing in Eq. (23)—both of which are of relativistic order and both happen to cancel exactly when the fully relativistic interaction (13) is considered.

We may further include the leading order relativistic corrections in the interaction if we retain higher order terms in Eq. (13). To this end, the relativistically extended light-matter interaction correct to order $(1/c)^2$ is obtained by imposing the unitary transformation (16)–(18) to the general Hamiltonian (13). By comparing Eqs. (13) and (20) and including all the surviving $(1/c)^2$ corrections we finally arrive at

$$H = \frac{p^2}{2m} - \frac{p^4}{8m^3c^2} + V(\boldsymbol{r} + \boldsymbol{\alpha}) - \frac{q}{m}\boldsymbol{A}_0 \cdot \boldsymbol{p} + \frac{q^2}{4m^2c}\{A^2, \hat{\boldsymbol{k}} \cdot \boldsymbol{p}\}$$
$$- \frac{q}{2m^2c}\{\hat{\boldsymbol{k}} \cdot \boldsymbol{p}, \boldsymbol{A} \cdot \boldsymbol{p}\} + \frac{q}{4m^3c^2}\{\boldsymbol{A} \cdot \boldsymbol{p}, p^2\}$$
$$- \frac{q^2}{8m^3c^2}\{A^2, p^2\}, \tag{25}$$

which is valid up to but not including order $(1/c)^3$ corrections. Notice at this point that the two extra terms appearing in Eqs. (20) and (23) are not part of this equation, merely confirming that the alternative formulations (21) and (24) comply better with the theory of relativity. The result (25) is equivalent but not identical to the results derived recently in [20,24], the most important distinction being that the transformation (16)–(18) was not imposed in the previous works.

Inspecting the radius of convergence of the Maclaurin series expansion in Eq. (9), it is found that the semirelativistic approach (25) gives the leading order relativistic correction provided the conditions,

$$\frac{q^2A^2}{m^2c^2} < 1 \quad \text{and} \quad \frac{p^2}{m^2c^2} < 1, \tag{26}$$

are fulfilled throughout the laser-matter interaction. In its present form only relativistic corrections to the kinetic energy are accounted for by Eq. (25), and the usual spin-orbit coupling and Darwin terms, as well as the coupling of the electronic spin to the magnetic field, have not yet been considered. These terms may, however, be included in the theory in a consistent manner following the so-called Foldy-Wouthuysen transformation scheme applied on the Dirac equation [43–45]. While beyond the scope of the present work, it would be an interesting topic for future studies to investigate to what extent such a semirelativistic approach is able to also accommodate for spin dynamics in a correct manner.

## III. RESULTS AND DISCUSSION

We have now come to the point where we want to explicitly demonstrate the capability of the alternative formulation of the light-matter interaction, i.e., the power of the nonrelativistic Hamiltonian (24) in comparison with the standard formulation (8). However, in order to compare their respective results on

an equal footing, the two terms which were of relativistic order and correctly left out from the formulation in the transition from Eq. (20) to (21) had to be reintroduced, i.e., the Hamiltonian (23) is used for this particular analysis.

For simplicity, we here consider the x-ray regime and a hydrogen 1s electron exposed to a 1.36-keV laser pulse which was powered on and off over a period of 15 cycles. The laser pulse is modeled in terms of the vector potential,

$$\boldsymbol{A}_0(t) = \frac{E_0}{\omega}f(t)\sin\omega t\ \hat{\boldsymbol{u}}_p, \tag{27}$$

where $E_0$ is the electric-field strength at peak intensity, and $\hat{\boldsymbol{u}}_p$ is a unit vector pointing in the laser polarization direction. Furthermore, the function $f(t)$ determines the temporal shape of the pulse and is here taken to be a sine-squared function, i.e.,

$$f(t) = \begin{cases} \sin^2\left(\frac{\pi t}{T}\right), & 0 < t < T \\ 0, & \text{otherwise,} \end{cases} \tag{28}$$

where $T$ indicates the total duration of the pulse.

The TDSE in Eq. (1) is then solved numerically using spherical coordinates and the spectral method, with the wave function $\psi$ expanded in a sufficiently large set of both quasicontinuum (scattering) and bound eigenstates of the field-free hydrogen atom as obtained by diagonalizing its system Hamiltonian in a combined B-spline and spherical harmonics basis [46]. More details on the numerical implementation are given in [47]. Accurate numerical results were obtained with a finite radial grid extending to $r = |\boldsymbol{r}| = 66$ a.u., and with the maximum attainable kinetic energy of the electron in the restricted basis set truncated at 610 a.u. Moreover, the number of angular momentum pairs $(l, m)$ included in the expansion of the wave function was varied until convergence was achieved. Note that when going beyond the dipole approximation, the azimuthal symmetry of the problem is broken, which means that values of the magnetic quantum number $m$ running from $-l$ to $+l$ must be taken into consideration. In our study we aimed at comparing the rate of convergence of the calculations with respect to the number of angular momenta included.

The atom is assumed exposed to a laser pulse of peak intensity $1.26 \times 10^{22}$ W/cm$^2$, which corresponds to the value $E_0 = 600$ a.u. in Eq. (27). Furthermore, the value of $\omega = 50$ in atomic units. At this high laser intensity and short wavelength of the light, the dipole approximation is no longer valid and magnetic effects become important [24,34].

Having obtained the final wave function at the end of the laser pulse, the resulting angular- and energy-resolved probability density is obtained as

$$\frac{d^2P}{dkd\Omega} = \left|\sum_{lm}(-i)^l e^{i\sigma_l} Y_{lm}(\Omega)\langle\Phi^C_{klm}(\boldsymbol{r})\big|\psi(\boldsymbol{r}, t = T)\rangle\right|^2, \tag{29}$$

where atomic units have been used, $\psi(\boldsymbol{r}, t = T)$ is the wave function at the end of the laser pulse, $\Phi^C_{klm}(\boldsymbol{r})$ is the Coulomb wave function (normalized on the $k$ scale), $k = \sqrt{2E}$ is the wave number in atomic units, and $\sigma_l = \arg\Gamma(l + 1 - i/k)$ is the Coulomb phase shift.

The top panel of Fig. 1 shows the energy distribution of the emitted photoelectron as obtained by solving the TDSE with the Hamiltonian (23), and for three different choices for
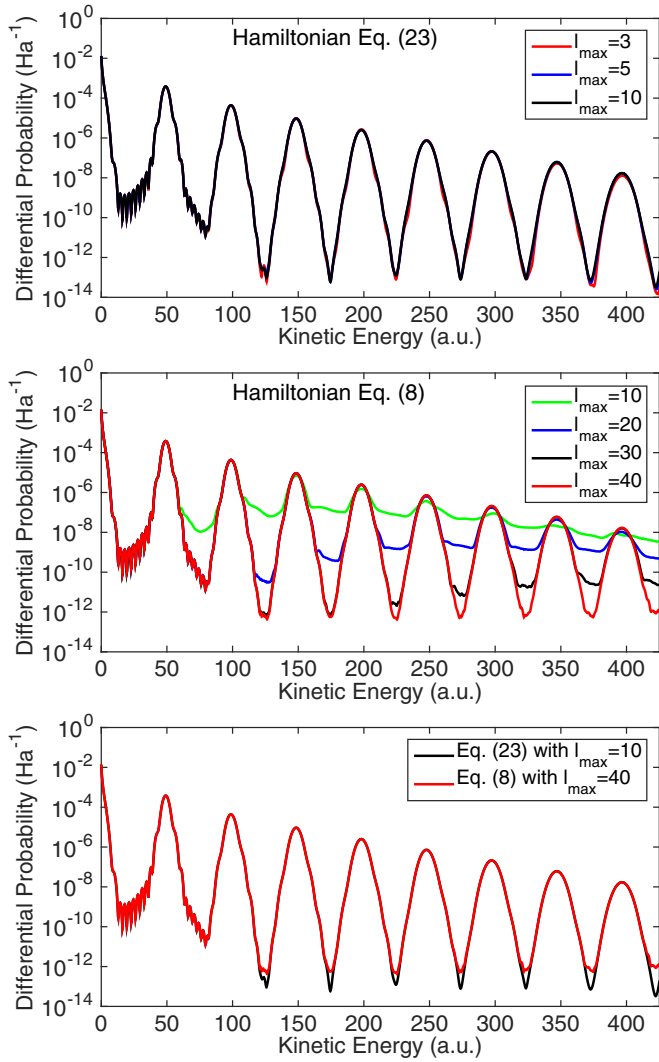
FIG. 2. Total population in (basis) states with angular momentum quantum number $l \geqslant 6$ as a function of time during the action of the laser pulse. The laser parameters are as in Fig. 1. Red (upper) line curve is the result obtained with the Hamiltonian (8). Black (lower) line curve is the result obtained with the Hamiltonian (23).

FIG. 1. Kinetic energy spectrum of the emitted photoelectron, as obtained by integrating Eq. (29) over all angles of emission, for a 15-cycle laser pulse with $\omega = 50$ a.u. and $E_0 = 600$ a.u. (Top panel) The beyond dipole result calculated using the Hamiltonian (23) and with $l_{max} = 3$ (red line), 5 (blue line), and 10 (black line), respectively. Note that the three results can hardly be distinguished on the scale of the figure. (Middle panel) The same result obtained with the Hamiltonian (8) and with $l_{max} = 10$ (green upper line), 20 (blue line, second from top), 30 (black line, third from top), and 40 (red lower line), respectively. (Bottom panel) A comparison of the results of Eqs. (8) and (23) with $l_{max} = 40$ (red upper line) and 10 (black lower line), respectively.

the truncation of the angular momentum quantum number $l$ in the expansion of the wave function. Specifically, we have set $l_{max} = 3$, 5, and 10, respectively. In total eight multiphoton peaks are depicted in the spectrum and only very small differences between the three calculated results are expressed. This finding merely reflects the fact that numerical calculations with the light-matter formulations (23) and (24) both converge very fast with respect to the total number of angular momenta included in the simulations.

The middle panel of Fig. 1 provides the corresponding result as obtained solving the TDSE with the conventional
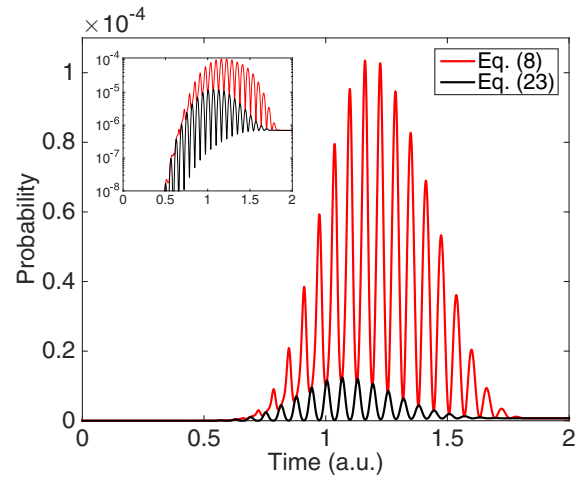
Hamiltonian (8), but now for relatively high values of the $l$ truncation. In this case $l_{max} = 10$, 20, 30, and 40, respectively. As it turns out, and in clear contrast to the upper panel result, the calculation now converges very slowly with respect to increasing number of angular momenta included in the basis expansion, and full convergence is difficult to achieve in practice. This is clearly manifested in the bottom panel of Fig. 1 showing a comparison of the result obtained by Eq. (23) and with $l_{max} = 10$, and Eq. (8) with $l_{max} = 40$, merely demonstrating that not even the $l_{max} = 40$ calculation seems to be fully converged for the higher electron energies.

The difference in the numerical performance of the two light-matter formulations (8) and (23) becomes even more evident when monitoring the temporal evolution of the population in high angular momentum states throughout the interaction. Figure 2 depicts the total probability of the electron being in an $l \geqslant 6$ state over the course of the pulse illumination. The figure reveals two important aspects of the time-dependent dynamics: First, the population in high lying $l$ states increases significantly during the interaction but ultimately declines to a rather small value at the very end of the laser interaction, and second, the increase in the population is much more pronounced when employing the interaction (8) rather than (23), the difference being almost an order of magnitude in favor of the formulation (23). Nonetheless, in an exact treatment and due to gauge invariance, the two calculations should of course converge to the very same $l$ distribution once the interaction with the laser field ceases. This fact is demonstrated in the logarithmic plot in the inset in Fig. 2, where it is indeed seen that the two curves converge to the same value as the field is turned off. Actually, the main reason why the alternative gauge (23) provides a numerically favorable formulation of the interaction is related to the fact that all components involving the momentum operator become constants of motion in the case of a free electron evolving in the external laser field, i.e., in the limit of vanishing potential $V$.
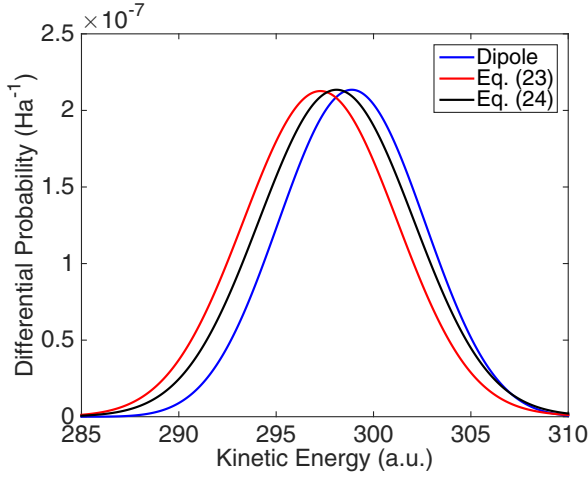
FIG. 3. A zoom of the six-photon peak of the kinetic energy spectrum of the emitted photoelectron for a 15-cycle laser pulse with $\omega = 50$ a.u. and $E_0 = 600$ a.u. The value of $l_{\max}$ was set to 10 in the calculations. Red (leftmost) line is the result obtained with Eq. (23) [or Eq. (8)]. Black (intermediate) line is the result obtained with Eq. (24). Blue (rightmost) line is the corresponding dipole approximation result.



FIG. 4. Same as Fig. 3, but a comparison of the relativistic and nonrelativsitic results. Red (leftmost) line is the nonrelativistic result obtained with Eq. (23) [or Eq. (8)]. Black (intermediate) line is the nonrelativistic result obtained with Eq. (24). Green (rightmost) line is the corresponding relativistic result obtained with Eq. (25) in the limit $\boldsymbol{A} \rightarrow \boldsymbol{A}_0$ and where the shifted potential (22) is expanded to first order in $1/c$.

Having settled the numerical superiority of the light-matter interaction formulation (23), which also applies to the formulation (24), we now present a comparison of the results obtained with the two Hamiltonians (23) and (24), respectively. The intent is to demonstrate the inaccuracy of the former. To this end, we consider the six-photon resonance peak in Fig. 1, and the result of the two respective calculations are shown in Fig. 3 together with the corresponding dipole approximation result. As it turns out, both the interactions (23) and (24) predict a shift of the resonance position towards lower electron energies with respect to the dipole result, effectively giving rise to a redshift of the multiphoton ionization spectrum. Furthermore, the former predicts a larger redshift than the latter.

As a matter of fact, the observed discrepancy between the results in Fig. 3 and between the data of Eqs. (23) and (24) in particular, provides some evidence that relativistic effects may play a certain role in the excitation dynamics. However, recently it was shown that such effects generally tend to produce a shift in the opposite direction, i.e., a blueshift of the spectrum with respect to the corresponding nondipole and nonrelativistic result [24]. Figure 4 depicts the relativistic result obtained with Eq. (25), and where the substitution $\boldsymbol{A} \rightarrow \boldsymbol{A}_0$ as well as the expansion (22) have been made in the system Hamiltonian. The corresponding nonrelativistic results given by Eqs. (23) and (24) are also shown for comparison. As it turns out, relativistic effects are responsible for a tiny shift of the position of the resonance towards higher energies, i.e., a blueshift. Furthermore, the net ionization yield is somewhat reduced as compared to its nonrelativistic counterparts. Noticing that the resonance is located at an even lower electron energy according to the calculation with Eq. (23) than with Eq. (24)—cf. red and black curve in Fig. 4—it is clear that the latter is more in line with the relativistic treatment. This merely suggests that the extra terms present in Eqs. (20) and
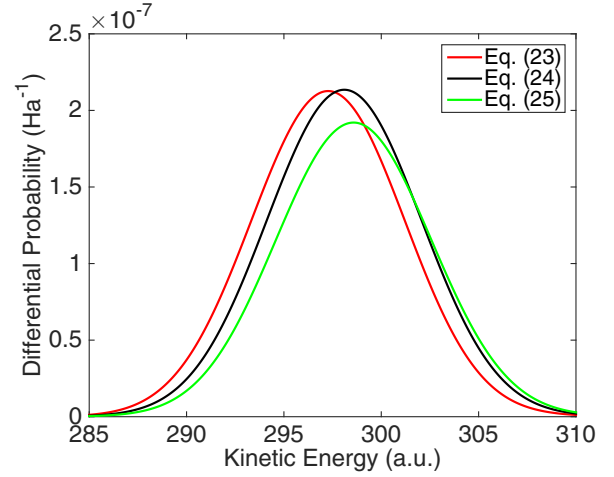
(23) are indeed superfluous, at best, and should be omitted in the general context.

In order to disentangle the role of the different terms of the Hamiltonian (25) on the underlying ionization dynamics, it may be useful to rewrite it on the following approximate form:

$$H = \frac{p^2}{2m} \underbrace{\left[ 1 - \frac{q^2 A_0^2}{2m^2 c^2} \right]}_{(I)} - \underbrace{\frac{p^4}{8m^3 c^2}}_{(II)} + V + \underbrace{\frac{q}{mc} \hat{\boldsymbol{k}} \cdot \boldsymbol{r} \, \nabla V \cdot \boldsymbol{A}_0}_{(III)}$$

$$- \frac{q}{m} \left[ 1 + \underbrace{\frac{\hat{\boldsymbol{k}} \cdot \boldsymbol{p}}{mc}}_{(IV)} - \underbrace{\frac{p^2}{2m^2 c^2}}_{(V)} \right] \boldsymbol{A}_0 \cdot \boldsymbol{p} + \underbrace{\frac{q^2}{2m^2 c} A_0^2 \hat{\boldsymbol{k}} \cdot \boldsymbol{p}}_{(VI)},$$

(30)

where we have explicitly made use of the expansion (22) for the shifted potential and the approximation $\boldsymbol{A} \simeq \boldsymbol{A}_0$ for the vector potential. Here, the three interaction terms (III), (IV), and (VI), respectively, are all of nonrelativistic origin and attributed to light propagation effects, like, for instance, the radiation pressure.

Now, returning to Fig. 4 and comparing the relativistic and nonrelativistic results, i.e., the green and black line curves, respectively, it is the term (I) in the Hamiltonian (30) that is responsible for the observed blueshift of the spectrum, while the decrease in the ionization yield is primarily attributed to the term (V), which effectively reduces the strength of the dipole interaction. Note that the term (I) is time dependent and only contributes during the time the laser field is on, i.e., it represents a temporal relativistic effect, in this case a transient relativistic mass shift [20]. Finally, the last term of relativistic origin, the permanent relativistic mass shift term (II), was found to have only minor influence on the predicted spectrum. This also applies to the electron's spin degree of freedom which was let out in the present analysis.
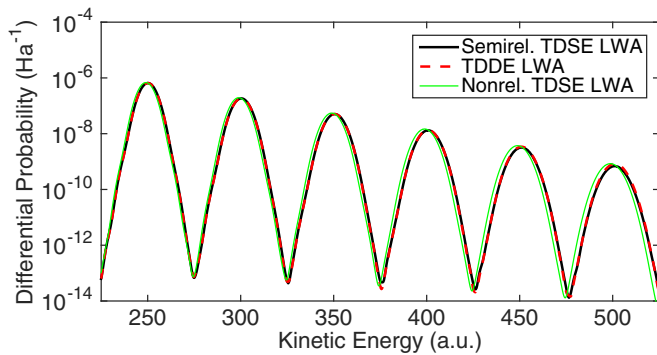
FIG. 5. Kinetic energy spectrum of the emitted photoelectron for the 15-cycle laser pulse with $\omega = 50$ a.u. and $E_0 = 600$ a.u. Multiphoton resonances corresponding to the net absorption of 5–10 photons from the field are depicted. (Dashed red line) The fully relativistic result obtained by solving the time-dependent Dirac equation (TDDE) within the long-wavelength approximation (LWA). (Thick black line) The corresponding semirelativistic LWA result obtained with the Hamiltonian (13) expanded to second order in $1/c$. (Thin green line) The nonrelativistic LWA result obtained with the Hamiltonian (13) expanded to first order in $1/c$.

In fact, it was recently verified by direct solutions of the time-dependent Dirac equation that the spin-orbit coupling term as well as the well-known Darwin term do not alter the kinetic-energy spectrum of the emitted photoelectron for the present range of field parameters [24], in compliance with the rule of thumb that spin-orbit effects are of less importance in atomic hydrogen than in its highly charged ion counterparts. For such multiply charged ions it has already been notified that the spin-orbit coupling may give rise to observable effects in intense laser-ion interactions [25,26].

As a final validation of the semirelativistic approximation (30) in describing the relativistic ionization dynamics of the atom, a one-to-one comparison with the exact result as obtained with the Klein-Gordon and/or Dirac equations would be in order. Unfortunately, these relativistic equations of motion are notoriously hard to solve numerically, primarily because they support both positive and negative energy solutions—resulting in a so-called stiff problem, but also due to the possible occurrence of spurious (artificial) states contaminating the spectrum. In addition, the Klein-Gordon equation is a second-order differential equation in time, and it does not necessarily preserve the norm of the wave function.

Nevertheless, recently a numerical application to solve the time-dependent Dirac equation (TDDE) within the so-called long-wavelength approximation (LWA) and the propagation gauge was developed [24,37]. In the semirelativistic approach, the LWA corresponds to letting $A(r, t) \rightarrow A_0(t)$ in each term in the Hamiltonian Eq. (13). For further details about the relativistic calculations with the Dirac equation the reader is referred to [20,24,37]. Figure 5 shows a comparison of the kinetic-energy spectrum as obtained by the TDDE and the result obtained with the TDSE and the semirelativistic Hamiltonian (13) expanded to second order in $1/c$. The corresponding nonrelativitic TDSE result is also shown. In all three cases, the LWA has been assumed. As expected, the figure shows that relativistic effects become increasingly
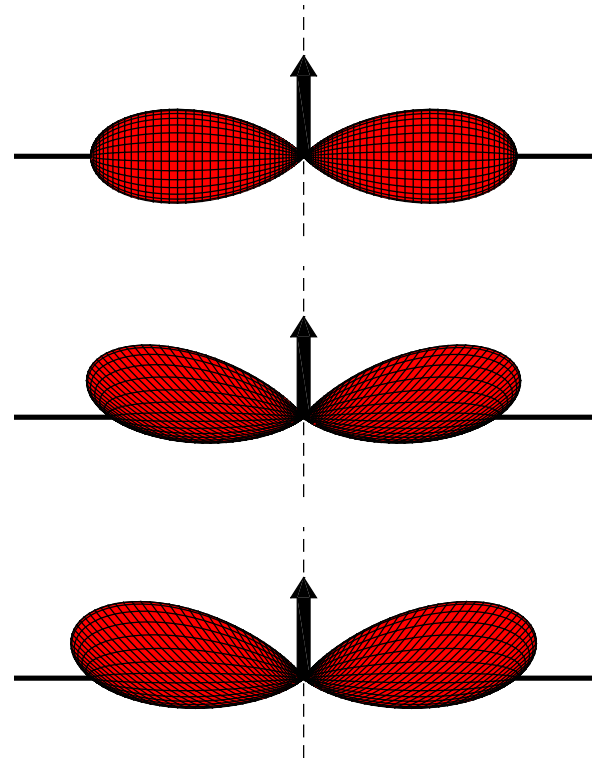


FIG. 6. Electron angular distributions, as obtained by integrating Eq. (29) over the electron energy interval $285 < E < 310$ a.u. (corresponding to the net absorption of six photons from the field; cf. Fig. 3). The laser pulse is assumed to be linearly polarized in the horizontal direction and propagating in the upward direction (indicated with an arrow in the figure), and the pulse parameters are as in Fig. 3. (Top panel) The (nonrelativistic) dipole approximation result. (Middle panel) The relativistic result obtained with the Hamiltonian (30). (Bottom panel) The corresponding nonrelativistic result obtained with the Hamiltonian (30) when disregarding all terms of relativistic order [i.e., the terms (I), (II), and (IV)] as well as the beyond-dipole terms (III) and (VI), i.e., only the nondipole term (IV) is accounted for in the calculation.

important with increasing kinetic energy of the photoelectron, and that these are manifested as a systematic shift of the resonance positions. Furthermore, and more importantly, the resulting close agreement between the TDDE and semirelativistic TDSE calculations clearly demonstrates the validity of the semirelativistic approach in describing the relativistic ionization dynamics.

Finally, in Fig. 6 we present (energy-integrated) angular distributions of the emitted photoelectron corresponding to the net absorption of six photons from the field; cf. the six-photon resonance in Figs. 3 and 4. The top panel shows the dipole approximation distribution, which is obviously symmetric with respect to the laser polarization axis. The middle panel depicts the fully relativistic and beyond-dipole result as obtained with the Hamiltonian (30), including all the terms (I–VI) in the interaction. Lastly, the bottom panel presents the result as obtained when disregarding all terms but the beyond-dipole term (IV) in the calculation, i.e., only the term (IV) is taken into consideration in addition to the ordinary dipole interaction.

As it turns out, the breakdown of the dipole approximation is manifested in Fig. 6 as a characteristic bending of the angular lobes in the laser propagation direction (upward), a finding that is in accordance with previously published results [34]. Furthermore, the close agreement found between the results in the middle and bottom panels in the figure simply suggests that relativistic effects are not of crucial importance when it comes to angular resolved (and energy-integrated) distributions. As such, it is the beyond-dipole term (IV) which represents by far the most important correction to the dipole approximation result in this case. Note further that since both these interactions scale linearly with $A_0$ [see Eq. (30)], the importance of the term (IV) with respect to the pure dipole interaction term is largely independent of the laser intensity and pulse duration, and hence the bending of the lobes is a general feature related to the photon energy and the acquired kinetic energy of the photoelectron rather than the laser intensity.

## IV. CONCLUSION

In this work, we have demonstrated that introducing spatial dependence in the vector potential in the $A \cdot p$ term in the standard nonrelativistic minimal-coupling formulation (2) can be problematic, in particular in the limit of intense laser fields, as this may lead to predictions that are in disagreement with relativity—even in field regimes where a nonrelativistic treatment is expected to be valid. With the intent to resolve this issue, we have here derived an alternative and relatively compact expression for the light-matter interaction Hamiltonian which in combination with the time-dependent Schrödinger equation effectively takes into account both beyond-dipole and relativistic effects. The corresponding nondipole nonrelativistic and relativistic formulations are given by Eqs. (21) and (25), respectively, in the present work. The formulation (21) is, although not relativistic in itself, formulated in concordance with relativity—with the consequence that superfluous interactions terms which otherwise would have appeared are consistently omitted. We have further demonstrated that these interaction forms are computationally much more efficient than the more standard formulations in describing atomic excitation and ionization dynamics in superintense laser fields. The reason why the representations (21) and (25) share such favorable numerical properties is that all components involving the momentum operator become approximately constants of motion in the strong coupling limit. Then, noticing that this finding is largely independent of the laser wavelength, this provides some evidence that the given numerical advantages also persist into the optical field regime.

[1] M. Ilchen, G. Hartmann, E. V. Gryzlova, A. Achner, E. Allaria, A. Beckmann, M. Braune, J. Buck, C. Callegari, R. N. Coffee *et al.*, Nat. Commun. **9**, 4659 (2018).

[2] C. T. L. Smeenk, L. Arissian, B. Zhou, A. Mysyrowicz, D. M. Villeneuve, A. Staudte, and P. B. Corkum, Phys. Rev. Lett. **106**, 193002 (2011).

[3] A. Ludwig, J. Maurer, B. W. Mayer, C. R. Phillips, L. Gallmann, and U. Keller, Phys. Rev. Lett. **113**, 243001 (2014).

[4] H. Zimmermann, S. Meise, A. Khujakulov, A. Magaña, A. Saenz, and U. Eichmann, Phys. Rev. Lett. **120**, 123202 (2018).

[5] S. Eilzer, H. Zimmermann, and U. Eichmann, Phys. Rev. Lett. **112**, 113001 (2014).

[6] A. Hartung, S. Eckart, S. Brennecke, J. Rist, D. Trabert, K. Fehre, M. Richter, H. Sann, S. Zeller, K. Henrichs *et al.*, Nat. Phys. **15**, 1222 (2019).

[7] B. Willenberg, J. Maurer, B. W. Mayer, and U. Keller, Nat. Commun. **10**, 5548 (2019).

[8] J. Maurer, B. Willenberg, J. Daněk, B. W. Mayer, C. R. Phillips, L. Gallmann, M. Klaiber, K. Z. Hatsagortsyan, C. H. Keitel, and U. Keller, Phys. Rev. A **97**, 013404 (2018).

[9] O. Hemmers, R. Guillemin, E. P. Kanter, B. Krässig, D. W. Lindle, S. H. Southworth, R. Wehlitz, J. Baker, A. Hudson, M. Lotrakul *et al.*, Phys. Rev. Lett. **91**, 053002 (2003).

[10] N. J. Kylstra, R. A. Worthington, A. Patel, P. L. Knight, J. R. Vázquez de Aldana, and L. Roso, Phys. Rev. Lett. **85**, 1835 (2000).

[11] M. Førre, J. P. Hansen, L. Kocbach, S. Selstø, and L. B. Madsen, Phys. Rev. Lett. **97**, 043601 (2006).

[12] H. Bachau, M. Dondera, and V. Florescu, Phys. Rev. Lett. **112**, 073001 (2014).

[13] M. Førre, S. Selstø, J. P. Hansen, and L. B. Madsen, Phys. Rev. Lett. **95**, 043601 (2005).

[14] S. Chelkowski, A. D. Bandrauk, and P. B. Corkum, Phys. Rev. Lett. **113**, 263005 (2014).

[15] S. Chelkowski, A. D. Bandrauk, and P. B. Corkum, Phys. Rev. A **92**, 051401(R) (2015).

[16] S. V. B. Jensen, M. M. Lund, and L. B. Madsen, Phys. Rev. A **101**, 043408 (2020).

[17] S. Selstø, E. Lindroth, and J. Bengtsson, Phys. Rev. A **79**, 043418 (2009).

[18] A. Di Piazza, C. Müller, K. Z. Hatsagortsyan, and C. H. Keitel, Rev. Mod. Phys. **84**, 1177 (2012).

[19] Y. I. Salamin, S. X. Hu, K. Z. Hatsagortsyan, and C. H. Keitel, Phys. Rep. **427**, 41 (2006).

[20] T. K. Lindblom, M. Førre, E. Lindroth, and S. Selstø, Phys. Rev. Lett. **121**, 253202 (2018).

[21] H. Bauke, H. G. Hetzheim, G. R. Mocken, M. Ruf, and C. H. Keitel, Phys. Rev. A **83**, 063414 (2011).

[22] T. Kjellsson, S. Selstø, and E. Lindroth, Phys. Rev. A **95**, 043403 (2017).

[23] M. S. Pindzola, J. A. Ludlow, and J. Colgan, Phys. Rev. A **81**, 063431 (2010).

[24] M. Førre, Phys. Rev. A **99**, 053410 (2019).

[25] S. X. Hu and C. H. Keitel, Phys. Rev. Lett. **83**, 4709 (1999).

[26] S. X. Hu and C. H. Keitel, Phys. Rev. A **63**, 053402 (2001).

[27] M. W. Walser, D. J. Urbach, K. Z. Hatsagortsyan, S. X. Hu, and C. H. Keitel, Phys. Rev. A **65**, 043410 (2002).

[28] S. X. Hu and C. H. Keitel, Europhys. Lett. **47**, 318 (1999).

[29] C. H. Keitel, P. L. Knight, and K. Burnett, Europhys. Lett. **24**, 539 (1993).

[30] N. J. Kylstra, A. M. Ermolaev, and C. J. Joachain, J. Phys. B: At. Mol. Opt. Phys. **30**, L449 (1997).

[31] I. A. Ivanov, Phys. Rev. A **91**, 043410 (2015).

[32] I. V. Ivanova, V. M. Shabaev, D. A. Telnov, and A. Saenz, Phys. Rev. A **98**, 063402 (2018).

[33] Y. V. Vanne and A. Saenz, Phys. Rev. A **85**, 033411 (2012).

[34] T. E. Moe and M. Førre, Phys. Rev. A **97**, 013415 (2018).

[35] M. Førre and A. S. Simonsen, Phys. Rev. A **93**, 013423 (2016).

[36] A. S. Simonsen and M. Førre, Phys. Rev. A **93**, 063425 (2016).

[37] T. Kjellsson, M. Førre, A. S. Simonsen, S. Selstø, and E. Lindroth, Phys. Rev. A **96**, 023426 (2017).

[38] M. Y. Ryabikin and A. M. Sergeev, Opt. Express **7**, 417 (2000).

[39] J. R. Vázquez de Aldana, N. J. Kylstra, L. Roso, P. L. Knight, A. Patel, and R. A. Worthington, Phys. Rev. A **64**, 013411 (2001).

[40] A. V. Kim, M. Y. Ryabikin, and A. M. Sergeev, Phys. Usp. **42**, 54 (1999).

[41] M. Y. Emelin and M. Y. Ryabikin, Phys. Rev. A **89**, 013418 (2014).

[42] S. Brennecke and M. Lein, J. Phys. B: At. Mol. Opt. Phys. **51**, 094005 (2018).

[43] L. L. Foldy and S. A. Wouthuysen, Phys. Rev. **78**, 29 (1950).

[44] Y. Hinschberger and P.-A. Hervieux, Phys. Lett. A **376**, 813 (2012).

[45] C. M. Soh, K. Younoussa, C. Bouri, M. G. K. Njock, and B. Piraux, Ann. Phys. **395**, 196 (2018).

[46] H. Bachau, E. Cormier, P. Decleva, J. E. Hansen, and F. Martín, Rep. Prog. Phys. **64**, 1815 (2001).

[47] M. Førre and A. S. Simonsen, Phys. Rev. A **90**, 053411 (2014).